Proflavine Acts as a Rev Inhibitor by Targeting the High-Affinity Rev Binding Site of the Rev Responsive Element of HIV-1†

Eric S. DeJong,‡ Chia-en Chang,‡ Michael K. Gilson, and John P. Marino*

Center for Advanced Research in Biotechnology of the University of Maryland Biotechnology Institute and the National Institute for Standards and Technology, 9600 Gudelsky Drive, Rockville, Maryland 20850

Received February 14, 2003; Revised Manuscript Received April 21, 2003

ABSTRACT: Rev is an essential regulatory HIV-1 protein that binds the Rev responsive element (RRE) within the *env* gene of the HIV-1 RNA genome, activating the switch between viral latency and active viral replication. Previously, we have shown that selective incorporation of the fluorescent probe 2-aminopurine (2-AP) into a truncated form of the RRE sequence (RRE-IIB) allowed the binding of an arginine-rich peptide derived from Rev and aminoglycosides to be characterized directly by fluorescence methods. Using these fluorescence and nuclear magnetic resonance (NMR) methods, proflavine has been identified, through a limited screen of selected small heterocyclic compounds, as a specific and high-affinity RRE-IIB binder which inhibits the interaction of the Rev peptide with RRE-IIB. Direct and competitive 2-AP fluorescence binding assays reveal that there are at least two classes of proflavine binding sites on RRE-IIB: a high-affinity site that competes with the Rev peptide for binding to RRE-IIB ($K_D \sim 0.1 \pm 0.05\ \mu$M) and a weaker binding site(s) ($K_D \sim 1.1 \pm 0.05\ \mu$M). Titrations of RRE-IIB with proflavine, monitored using ^{1}H NMR, demonstrate that the high-affinity proflavine binding interaction occurs with a 2:1 (proflavine:RRE-IIB) stoichiometry, and NOEs observed in the NOESY spectrum of the 2:1 proflavine•RRE-IIB complex indicate that the two proflavine molecules bind specifically and close to each other within a single binding site. NOESY data further indicate that formation of the 2:1 proflavine•RRE-IIB complex stabilizes base pairing and stacking within the internal purine-rich bulge of RRE-IIB in a manner analogous to what has been observed in the Rev peptide•RRE-IIB complex. The observation that proflavine competes with Rev for binding to RRE-IIB by binding as a dimer to a single high-affinity site opens the possibility for rational drug design based on linking and modifying it and related compounds.

In human immunodeficiency virus type 1 (HIV-1),[1] interaction between the regulatory protein Rev and a portion of the *env* gene within the RNA genome, the so-called Rev responsive element (RRE), is critical for viral replication (*1*−*5*). During the late phase of HIV-1 infection, Rev binds unspliced and incompletely spliced viral mRNAs and mediates the transport of these mRNAs from the nucleus into the cytoplasm for translation into viral proteins (e.g., Gag, Gag-pol, and Env) essential for viral particle assembly. Since Rev protein binding to viral mRNA at the RRE is essential for HIV replication, acting as a crucial switch between viral latency and active viral replication, the development of inhibitors of this critical interaction could provide the basis for new drug therapies against HIV-1 infection. In fact, a number of biological agents directed against RRE or Rev have been shown to inhibit HIV-1 replication *in vivo* (*6*, *7*), thus demonstrating that this viral specific RNA−protein (RNP) complex is a valid and viable target for antiviral agents.

To date, only a few small organic compounds have been reported which block the Rev•RRE interaction *in vitro* with inhibition constants in the nano- to micromolar range. Among these compounds are a number of aminoglycoside antibiotics that have been shown through *in vitro* binding assays to effectively compete with Rev for binding to RRE (*8*−*12*). Since aminoglycosides represent a rare example of a small molecule class that is known to selectively target rRNA *in vivo*, a number of studies have focused on attempting to modify these compounds to enhance their specificity for RRE through directed and combinatorial chemical approaches (*13*−*16*). For example, conjugation of neomycin B with an acridine derivative results in a significantly enhanced affinity for RRE (*14*). Of the aminoglycoside antibiotics assayed *in vitro*, however, only neomycin B has also exhibited antiviral activity in cell-based assays (*8*), and it is effective at only relatively high concentrations (>100 μM). Although the

† This work was supported by NIH Grant GM59107 to J.P.M. and Grant GM61300 to M.K.G. E.S.D. acknowledges a National Research Council postdoctoral fellowship. NMR instrumentation was supported in part by the W. M. Keck Foundation.

* To whom correspondence should be addressed. Telephone: (301) 738-6160. Fax: (301) 738-6255. E-mail: marino@carb.nist.gov.

‡ These authors contributed equally to this work.

[1] Abbreviations: HIV-1, human immune deficiency virus type 1; RRE-IIB, truncated version of the Rev responsive element corresponding to stem−loop IIB of the full-length 234-nucleotide sequence; Tris-HCl, tris(hydroxymethyl)aminomethane chloride; RNP, RNA−protein; PAGE, polyacrylamide gel electrophoresis; DEPC, diethyl pyrocarbonate; 2-AP, 2-aminopurine; NMR, nuclear magnetic resonance; 1D, one-dimensional; 2D, two-dimensional; NOESY, nuclear Overhauser effect spectroscopy; ROESY, rotating Overhauser effect spectroscopy; TOCSY, total correlation spectroscopy; COSY, correlation spectroscopy; HPLC, high-performance liquid chromatography; MALDI-TOF MS, matrix-assisted laser desorption ionization time-of-flight mass spectrometry.

10.1021/bi034252z CCC: $25.00
Published on Web 06/10/2003

inhibition elicited by neomycin B has focused attention on this compound as a lead in the search for new antiviral agents, its molecular complexity, toxicity, poor oral adsorption, and modest specificity make it a less than ideal lead candidate. A second group of compounds shown to bind RRE *in vitro* and inhibit its interaction with Rev are the diphenylfuran cations (*17*−*19*). Some of these unfused, aromatic cationic compounds bind tightly to RRE and block the Rev·RRE complex at concentrations as low as 0.1 μM. A detailed biochemical and structural analysis of one high-affinity RRE binding compound from the diphenylfuran cations, a tetracation heterocycle containing a phenylfuranbenzimidazole aromatic system, has revealed that this molecule binds as a dimer to the minor groove of the purine-rich internal bulge of RRE-IIB with pronounced selectivity (*20*).

In addition to the focused studies on aminoglycosides and diphenylfuran cations, a few *in vitro* and cell-based assays have also been developed to facilitate high-throughput screening directed at the discovery of novel modulators of the Rev·RRE interaction. In one recent study in which more than 500 000 compounds were randomly screened using a scintillation proximity assay, diphenylfuran cations were again identified as antagonists of the Rev·RRE interaction, along with several new classes of antagonists and two chemical classes of Rev·RRE enhancers (*21*). Despite this and other examples of the successful identification of small molecules that can block the RRE·Rev interaction *in vitro* with modest inhibition constants (K_i < 1 μM), as well as the clear potential of the RRE·Rev interaction as a therapeutic target, so far no compounds have advanced to the clinic. It is therefore of continued interest to search for new small molecules that bind with high affinity to RRE and inhibit its interaction with Rev. More generally, identification and characterization of novel small molecules that bind RRE will also expand our currently limited knowledge of the molecular repertoire available for specific, high-affinity small molecule interactions with RNA.

Stem−loop IIB (RRE-IIB) within RRE contains a purine-rich internal bulge structure that has been identified as a high-affinity Rev binding site (*22*, *23*). Rev, as well as small peptides containing a 17-amino acid arginine-rich region of Rev (amino acids 34−51), specifically binds RRE-IIB with nanomolar affinity (*24*−*30*), making this stem−loop motif a useful model system for *in vitro* studies. We have shown previously that selective incorporation of the fluorescent base analog 2-aminopurine (2-AP) into RRE-IIB at positions A68 and U72 (Figure 1) can provide sensitive probes for detecting binding of both Rev peptide and small molecule ligands (*31*). The sensitivity of the quantum yield of 2-AP to its microenvironment allows binding to be detected through direct contact, as well as indirectly through conformational changes in the RNA that may accompany the interaction with a ligand (*31*−*33*). Nuclear magnetic resonance (NMR) methods were also demonstrated to provide rapid structural information for qualitative characterization of the interaction of aminoglycosides with RRE-IIB (*31*). Using similar fluorescence and NMR methods, proflavine has been identified in this study, through a limited screening of a selected set of small heterocyclic compounds, as a specific and high-affinity binder of RRE-IIB. Proflavine is also shown to compete directly with the arginine-rich Rev peptide for binding to RRE-IIB. Furthermore, proflavine is found to interact with

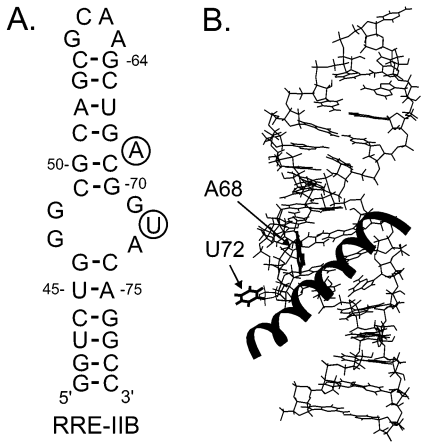

FIGURE 1: (A) Basic sequence and secondary structure of the 34mer RNA stem−loop RRE-IIB of the Rev responsive element (RRE) used in the NMR and fluorescence measurements. Residues A68 and U72 that are substituted with the fluorescent nucleotide analogue of adenosine, 2-aminopurine (2-AP), to generate constructs RRE-68ap and RRE-72ap, respectively, used in the fluorescence binding assays are circled. (B) NMR-determined structure of RRE-IIB in complex with an 18-amino acid (amino acids 34−51) arginine-rich peptide derived from Rev (*28*). Highlighted in bold are residues A68 and U72 located within the high-affinity Rev binding site, which have been substituted with 2-AP to form constructs RRE-72ap and RRE-68ap, respectively.

a 2:1 (proflavine:RRE-IIB) stoichiometry with two molecules bound in a specific conformation and close to each other in a single high-affinity site. Interestingly, formation of the 2:1 proflavine·RRE-IIB complex results in a stabilization of the base pairing and stacking within the internal purine-rich bulge of RRE-IIB, which forms the core of the previously identified high-affinity Rev binding site. A similar, but more pronounced, stabilizing effect on the RNA conformation of RRE-IIB has been observed in the Rev peptide·RRE-IIB complex. On the basis of our findings, we propose a model for the competitive, high-affinity binding interaction of proflavine with RRE-IIB and suggest possibilities for enhancing specificity and activity through chemical modification of it and related heterocyclic aromatic compounds.

MATERIALS AND METHODS[2]

Materials. Compounds of low molecular weight were purchased from Sigma-Aldrich (St. Louis, MO) and used without further purification. All other buffers and reagents were of the highest quality commercially available and were used without further purification.

Criteria Used To Select Compounds for Screening. The selection of a set of compounds to test for potential binding to the RRE-IIB stem−loop region was guided in part by knowledge of the general molecular features that are likely to promote RNA binding. For example, the ability to adopt a positive charge was assumed to be important for binding since a positively charged ligand could replace some of the mobile cations it displaces upon binding to the RNA. The potency of the polycationic aminoglycoside antibiotics, such

[2] Certain commercial equipment, instruments, and materials are identified in this paper to specify the experimental procedure. Such identification does not imply recommendation or endorsement by the National Institute of Standards and Technology, nor does it imply that the material or equipment identified is necessarily the best available for the purpose.

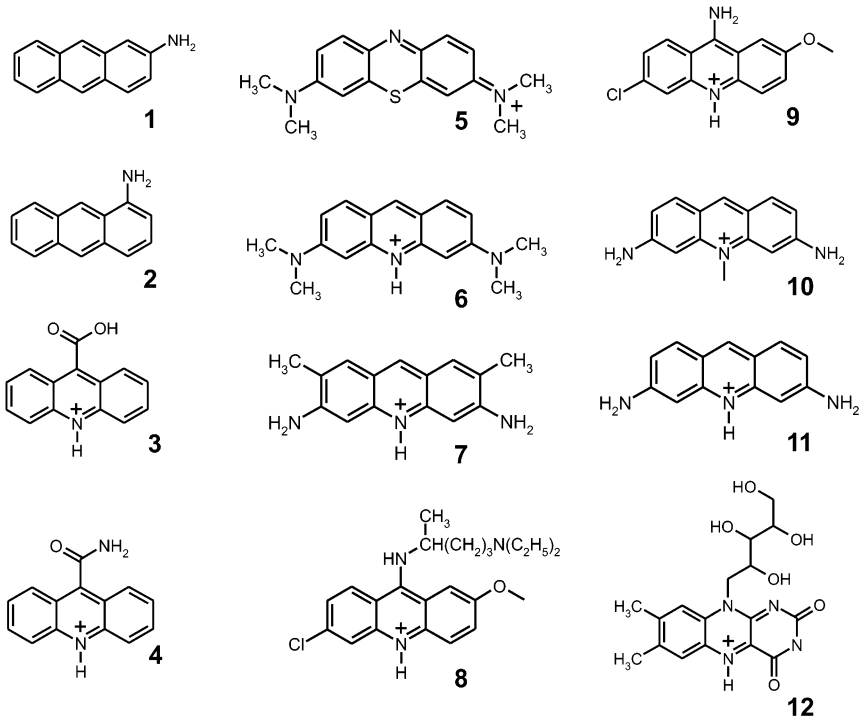

FIGURE 2: Structures of the polycyclic aromatic compounds tested for binding to RRE-IIB using the 2-AP fluorescence assay: (**1**) 1-anthramine, (**2**) 2-anthramine, (**3**) 9-acridinecarboxylic acid, (**4**) 9-acridinecarboxyamine, (**5**) methylene blue, (**6**) acridine orange, (**7**) acridine yellow, (**8**) quinacrine, (**9**) 9-amino-6-chloro-2-methoxyacridine, (**10**) 3,6-diamino-10-methylacridinium chloride, (**11**) proflavine, and (**12**) riboflavin. Charges on the molecules are shown as expected at neutral pH.

as neomycin B, is consistent with this view (*11*, *12*, *15*, *34*−*36*), as is the observation that neomycin B displaces Mg^{2+} ions upon binding tRNA in a crystal structure of the antibiotic−RNA complex (*37*). The selection was further focused on hydrophobic cationic molecules since it was reasoned that these molecules, unlike aminoglycosides, would be more readily absorbed through membranes and therefore any initial "hits" would be automatically biased toward better lead compounds for therapeutic development. Further guidance for database searching was derived from previous work which demonstrated that conjugating the aromatic heterocycle acridine or derivatives thereof to polycations enhanced the affinity of these compounds for the transactivation region (TAR) regulatory RNA element of HIV-1 (*38*). In addition, the antimalarial drug quinacrine, which possesses an acridine-like moiety, is known to bind RNA (*39*, *40*) and DNA (*41*) and, encouragingly, is a safe and effective therapeutic. On the basis of these considerations, acridine was used as the basis of similarity and substructure searches in the National Cancer Institute (NCI) database and in the Sigma-Aldrich catalog. These searches generated a large set of molecules from which an initial subset of compounds (Figure 2) was selected for testing, based on further considerations of cost, availability, toxicity, and solubility.

RNA and Peptide Synthesis. Unlabeled and uniformly ^{15}N-labeled RRE-IIB (Figure 1A) stem−loop motifs encompassing the high-affinity Rev binding site were prepared by *in vitro* T7 polymerase runoff transcription reactions according to the method described by Milligan and Uhlenbeck (*42*) using synthetic DNA templates prepared by solid-phase synthesis. Unlabeled RNA was synthesized using NTPs purchased from Amersham Biosciences (Piscataway, NJ). Uniformly ^{15}N-labeled NTPs were harvested from *Escherichia coli* grown on M9 minimal media using $^{15}NH_4Cl$ purchased from Spectral Stable Isotopes (Columbia, MD) as the sole nitrogen source and prepared using published protocols (*43*, *44*). The two RRE-IIB constructs, specifically labeled with the fluorescent nucleotide analogue 2-aminopurine (2-AP) at positions A68 and U72 (RRE-68ap and RRE-72ap, respectively), were prepared using solid-phase synthesis and phosphoramidites purchased from Glenn Research (Sterling, VA). RNA prepared by either *in vitro* T7 polymerase runoff transcription reactions or solid-phase synthesis was purified using preparative-scale denaturing polyacrylamide gel electrophoresis (PAGE), electroeluted from excised bands, and desalted by extensive dialysis against sterile, diethyl pyrocarbonate (DEPC)-treated ddH_2O followed by buffer A [1 mM cacodylate (pH 6.5) and 25 mM NaCl]. The RNA concentration was determined by measuring the absorbance at 260 nm using an extinction coefficient of 322.9 mM^{-1} cm^{-1} for RRE-IIB.

The 22-amino acid (Suc-TRQARRNRRRRWRERQR-AAAAK) arginine-rich peptide used in this study was derived from the Rev protein and previously shown to interact with high affinity with RRE-IIB (*25*, *27*, *29*). The peptide was synthesized by Bio Synthesis, Inc. (Lewisville, TX), and purified using C-18 reversed-phase high-pressure liquid chromatography (HPLC) to a final purity of >95%. Matrix-assisted laser desorption ionization time-of-flight mass spectrometry (MALDI-TOF MS) (Perceptive Biosystems, Framington, MA) analysis gave a MW (MH^+) of 2950.2. The Rev peptide concentration was determined from its extinction coefficient at 280 nm (5.6 mM^{-1} cm^{-1}).

Steady-State Fluorescence Measurements of Rev Peptide and Ligand Binding to 2-AP-Labeled RRE-IIB. The fluorescence of the selectively 2-AP-labeled RRE-IIB samples (150 μL) was measured at 10 °C on either a SPEX Fluoromax-2 or Fluoromax-3 spectrofluorometer (Instruments SA, Edison,

NJ) using a 0.3 cm square cuvette. Emission spectra were recorded over the wavelength range of 330−450 nm with an excitation wavelength of 310 nm. The spectral excitation and emission band-pass was 5 nm for all spectra. Fluorescence binding measurements were carried out in buffer B [140 mM NaCl, 5 mM KCl, 1 mM $MgCl_2$, 1 mM $CaCl_2$, and 20 mM HEPES (pH 7.4)]. Heterocyclic compounds screened for high-affinity binding to RRE-IIB were titrated into fixed concentrations of either RRE-72ap or RRE-68ap, and changes in 2-AP fluorescence were monitored at the fluorescence emission maximum of 371 nm. Observation of a 2-AP fluorescence change corresponding to a single-site binding mode for a compound was fit using eq 1:

$$F = -[(F_o - F_f)/(2[\mathrm{RRE}]_{tot})] \times [b - \sqrt{b^2 - 4[\mathrm{L}]_{tot}[\mathrm{RRE}]_{tot}}] + F_o \quad (1)$$

$$b = K_d + [\mathrm{L}]_{tot} + [\mathrm{RRE}]_{tot}$$

where F_o and F_f are the initial and final fluorescence intensities, respectively, $[\mathrm{RRE}]_{tot}$ is the total RRE concentration, and $[\mathrm{L}]_{tot}$ is the total ligand concentration.

Competitive displacement assays were performed to assay for inhibition of Rev peptide binding by one of the small molecule compounds, proflavine, which was found to interact with RRE-IIB in the direct binding assays. These experiments were carried out using low salt (buffer A), as well as more saline buffer conditions (buffer B). For these experiments, a solution of 2-AP-labeled RRE was incubated with a fixed concentration of proflavine (or Rev peptide), and the fluorescence change was followed as increasing amounts of competing Rev peptide (or proflavine) was added to the solution. The fluorescence emission intensities at 371 nm as a function of total added ligand concentration were fit to a given molecular mechanism by nonlinear least-squares regression using *DynaFit* (*45*). This program determines the composition of complex mixtures at equilibrium by simultaneously solving the nonlinear equations for mass balance of the component species. Thus, the observed fluorescence changes could be fit to a number of defined models to allow the determination of the simplest best-fit model for a given system. The fluorescence emission intensities at 370 nm as a function of total added ligand concentration were fit to a given molecular mechanism by nonlinear least-squares regression using *DynaFit* (*40*). Details of individual displacement experiments are described in the figure legends and Results.

Error Analysis. The reported errors are the standard uncertainties of the data from the best-fit theoretical curves. This method assumes that the standard uncertainty of the measurement is approximated by the standard deviation of the points from the fitted curve.

NMR Spectroscopy. NMR samples were extensively dialyzed against a 10 mM d_{11}-Tris buffer at pH 6.9 and 100 mM NaCl (NMR buffer), lyophilized to dryness, and resuspended in either a 90% H_2O/10% D_2O mixture or 100% D_2O to a final volume of 300 μL in Shigemi limited volume NMR tubes (Shigemi, Inc., Allison, PA). NMR spectra were recorded on either Bruker AVANCE 600 MHz or AVANCE 500 MHz spectrometers (Bruker Instruments, Billerica, MA) equipped with triple-resonance ^1H, ^{13}C, ^{15}N triple-axis gradient probes.

One-dimensional (1D) proton spectra were collected at 283, 288, 293, and 298 K using a water flip-back Watergate pulse sequence (*46*, *47*) with a sweep width of 12 500 Hz, 4096 complex points, and 256 scans and processed using 5 Hz line broadening in XWINNMR version 2.6 (Bruker Instruments). Two-dimensional (2D) TOCSY and NOESY spectra were recorded at 283, 288, 293, and 298 K using water flip-back Watergate water suppression (*47*). All TOCSY spectra were collected with a mixing time of 25 ms and sweep widths of 7200 Hz in both dimensions, 2048 and 200 complex data points in t_2 and t_1, respectively, and 80 scans per increment. All NOESY spectra were collected using a T_{NOE} mixing time of 250 ms and sweep widths of 13 200 Hz in both dimensions, 4096 and 384 complex data points in t_2 and t_1, respectively, and 208 scans per increment. A 2D ROESY experiment was carried out at 283 K using a T_{ROE} mixing time of 150 ms, with sweep widths of 7184 and 6000 Hz and 2048 and 160 complex data points in t_2 and t_1, respectively, and 128 scans per increment. $^{2h}J_{NN}$ COSY spectra were recorded at 283 K as previously described (*48*), with sweep widths of 12 000 Hz in t_1 and 7000 Hz in t_2, 4096 and 64 complex data points in t_2 and t_1, respectively, and 256 scans per increment. 2D data sets were processed using nmrPipe (*49*) software on a LINUX/PC workstation. TOCSY spectra were apodized using 65°- and 45°-shifted sine-squared bell functions over 512 and 200 complex points in the t_2 and t_1 dimensions, respectively, and zero-filled to 1024 real points in both dimensions. NOESY spectra were apodized using 65°- and 45°-shifted sine-squared bell functions over 512 and 384 complex points in the t_2 and t_1 dimensions, respectively, and zero-filled to 1024 real points in both dimensions.

RESULTS

Screening for Small Aromatic Molecules that Bind RRE-IIB. On the basis of considerations of the general molecular features likely to promote binding to RNA as well as favorable drug-like chemical properties, acridine was used as the basis of similarity and substructure searches of compound libraries. An initial group of compounds (Figure 2), selected from a much larger set of molecules that fit the crude selection criteria, was tested for binding to RRE-IIB (Figure 1) by monitoring changes in the 2-AP fluorescence emission that resulted from the titration of a compound with a fixed concentration of either RRE-68ap or RRE-72ap (*31*). Table 1 provides a summary of the results of the direct binding experiments with the individual compounds. Of the compounds initially screened, several induced significant quenching of the 2-AP fluorescence emission in both RRE-68ap and RRE-72ap, indicating that these compounds interact directly with RRE-IIB. As indicated in Table 1, there appears to be a correlation between net positive charge on the ring system and the extent of binding, as would be expected given the polyanionic nature of RNA.

In the titration series, proflavine (**11**) and acridine orange (**6**) showed the most significant quenching of fluorescence (Table 1), with decreases of 80% of the original fluorescence emission of both the RRE-68ap and RRE-72ap constructs after titration to a concentration of 5 μM compound. Figure 3 shows the results of the two titrations of proflavine with RRE-72ap and RRE-68ap. The resulting fluorescence changes for RRE-72ap (Figure 3A) and RRE-68ap (Figure 3B)

Table 1: Fluorescence Response from the Titration of the 12 Compounds in Figure 2 with a Fixed Concentration of RRE-68ap and RRE-72ap

compound[a]	net charge	RRE-68ap 1 μM	RRE-68ap 5 μM	RRE-72ap[c] 1 μM	RRE-72ap[c] 5 μM
1-anthramine (**1**)	zero	↔	↔	↔	↔
2-anthramine (**2**)	zero	↔	↔	↔	↔
9-acridinecarboxylic acid (**3**)	positive	↔	↔	↔	↔
9-acridinecarboxyamine (**4**)	positive	↔	↑	↔	↔
methylene blue (**5**)	zwitter-ionic	↓↓	↓↓↓	↓	↓↓
acridine orange (**6**)	positive	↓↓	↓↓↓	↓↓	↓↓↓↓
acridine yellow G (**7**)	positive	nd[b]	nd[b]	↓↓	↓↓↓
quinacrine (**8**)	positive	↔	↓↓	↔	↓↓
9-amino-6-chloro-2-methoxy-acridine (**9**)	positive	↓	↓↓	↓	↓↓
3,6-diamino-10-methyl-acridinium chloride (**10**)	positive	↓↓	↓↓↓	↓↓	↓↓↓
proflavine (**11**)	positive	↓↓	↓↓↓	↓↓	↓↓↓↓
riboflavin (**12**)	positive	↔	↔	↔	↔

[a] The compounds were titrated independently against 100 nM RRE-68ap and 100 nM RRE-72ap in buffer B at 10 °C. Each ↑ or ↓ represents an increase or decrease, respectively, in the emission intensity at 371 nm of 20% relative to the initial observed fluorescence for the RNA sample alone. Fluorescence changes at compound concentrations of 1 and 5 μM are shown. The horizontal double-headed arrows (↔) represent changes in fluorescence of less than 10%. [b] Not determined. [c] A binding constant was fit using a single-site binding model (Figure 3) for the titrations with RRE-72ap where a significant fluorescence change was observed.

observed as a result of titration with proflavine (**11**) were fit assuming a single binding mode with eq 1, and K_D values of 1.15 ± 0.12 and 1.05 ± 0.05 μM were determined, respectively. Since the binding event detected by the RRE-72ap and RRE-68ap samples has the same affinity, it appears that these probes are detecting the same interaction in both experimental titrations. Similarly, a binding constant ($K_D \sim$ 1.53 ± 0.08 μM) could be determined for acridine orange (**6**) by fitting the titration data (data not shown) to a single binding mode (eq 1).

The quenching of 2-AP fluorescence, which resulted in all cases where a compound induced any fluorescence response, suggests that the 2-AP probes become more stacked and/or occupy more hydrophobic environments in these RNA−small molecule complexes. Such quenching can result from either direct interaction or stacking of the aromatic compounds with the 2-AP bases or from an allosteric conformational perturbation in the RNA structure which results in the stacking of 2-AP with surrounding RNA bases. In contrast to the general observation of quenching of fluorescence in the titrations of some heterocyclic compounds with 2-AP-labeled RRE, neither the anthramine compounds nor the acridine derivatives functionalized at position 9 of the tricyclic ring induced significant fluorescence responses in titrations with either RRE-68ap or RRE-72ap. In addition, riboflavine (**12**) and quinacrine (**8**), which have bulky substituents at position 9 of the tricyclic ring, also had little or no effect on the fluorescence emission of RRE-68ap and RRE-72ap in titrations. These results are consistent with a role for electrostatic interactions in the binding reaction and also suggest that substitutions at position 9 in the ring may lead to steric clashes with the RNA. Although we cannot be absolutely certain that these inactive compounds do not bind to RRE-IIB, it is clear that any interaction of these compounds that occurs within the titration range of 0−10 μM does not either directly or indirectly affect the conformation of the high-affinity Rev binding site of the RRE structure in a way on which the 2-AP probe reports in either RRE-68ap or RRE-72ap.

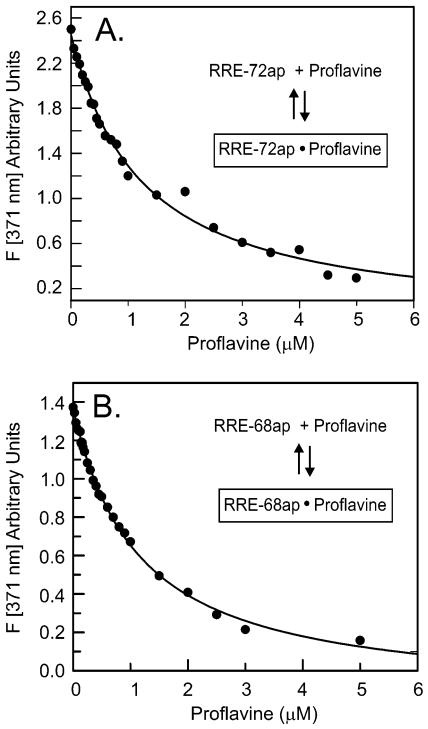

FIGURE 3: Fluorescence changes accompanying titration of 2-AP-labeled RRE-IIB with proflavine. (A) Titration of 100 nM RRE-72ap with increasing concentrations of proflavine in buffer B at 10 °C. The relative fluorescence increase at 371 nm as a function of total proflavine concentration is plotted, and the data are fit using a single-site binding model (K_D = 1.15 ± 0.12 μM). (B) Titration of 100 nM RRE-68ap with increasing concentrations of proflavine in buffer B at 10 °C. Relative fluorescence changes at 371 nm for 100 nM RRE-68ap as a function of total proflavine concentration are plotted, and the data are fit using a single-site binding model (K_D = 1.07 ± 0.05 μM). The species that is directly detected in each experiment is marked with a box in each panel.

Detection of Formation of the Proflavine·RRE Complex Using NMR Spectroscopy. As a secondary approach to the 2-AP fluorescence binding assay, the analysis of complexes formed between RRE-IIB and selected small molecule compounds was pursued using complementary ^{1}H NMR experiments. The two compounds which showed the most significant 2-AP fluorescence quenching and the tightest binding interactions, proflavine and acridine orange, were initially chosen for NMR analysis.

Using NMR experiments, the formation of a stable, soluble complex of proflavine with RRE-IIB at NMR concentrations could readily be monitored. Figure 4 shows the expansion of the imino proton region of 1D proton NMR spectra taken at points along the titration of proflavine with 100 μM RRE-IIB at 283 K in NMR buffer. The NMR spectra were monitored to detect any changes in the exchangeable imino proton resonances associated with proflavine binding. Over the course of the titration, several imino proton resonances diminished in intensity while new imino proton resonances were observed. These observations indicated a slow exchange between two conformational states of the RRE-IIB stem−loop motif: free RRE-IIB and RRE-IIB with proflavine occupying a single, specific binding site. In the titration,

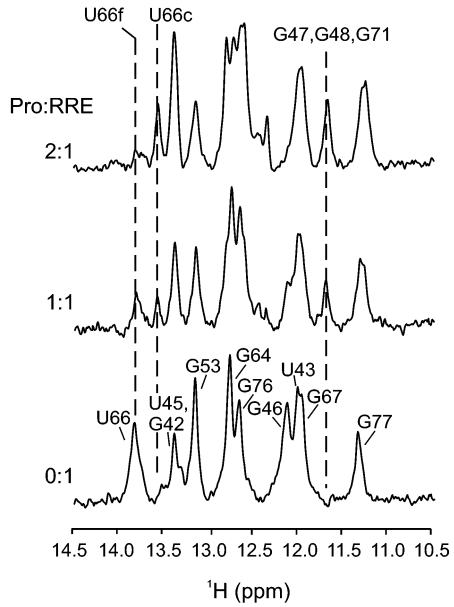

FIGURE 4: Titration of RRE-IIB with proflavine resulting in the formation of a specific proflavine·RRE-IIB complex. Expansions of the imino region (from 14.5 to 10.5 ppm) of 1D proton spectra collected at 283 K are shown for free RRE-IIB (bottom spectrum), RRE-IIB in the presence of 1 molar equiv of proflavine (middle spectrum), and RRE-IIB in the presence of 2 molar equiv of proflavine (top spectrum). Molar ratios of proflavine to RNA are indicated with each trace, and assignments for free RRE-IIB are given (*27*). The imino position of residue U66 is highlighted to demonstrate that the proflavine·RRE-IIB complex is in slow exchange with free RRE-IIB. As proflavine is titrated with RRE-IIB, the magnitude of the imino resonance signal for U66 in the free RRE-IIB state, labeled U66f, decreases while the magnitude of the corresponding U66 signal for the complex, denoted U66c, increases. No evidence for stable formation of an intermediate with a single proflavine molecule bound to RRE-IIB can be detected from the NMR spectra, indicating that binding of the two molecules of proflavine to RRE-IIB is highly cooperative. The imino resonance signals ambiguously assigned to residues G47, G48, and G71, which are not observed in the free RRE-IIB spectrum but found to increase in intensity over the course of the titration, are also highlighted to indicate evidence of RRE-IIB bulge stabilization in the complex.

proflavine was added until all new imino signals stopped increasing in intensity and all diminishing imino proton resonances were no longer observable. Upon completion of the titration, an apparent stoichiometry of 2:1 (proflavine:RRE-IIB) was found for the proflavine·RRE-IIB complex. In addition, since only one set of new imino proton signals was observed during the course of the titration, the binding of two proflavine molecules to RRE-IIB appears to be highly cooperative, with no evidence of a stable intermediate complex formed between one proflavine and RRE-IIB. The titration of proflavine with RRE-IIB was repeated at several higher temperatures (288, 293, and 298 K), and at each temperature, the final stoichiometric ratio of proflavine to RRE-IIB that was achieved was found to be 2:1 (data not shown). However, some of the imino protons associated with the purine-rich internal bulge region of RRE-IIB in the proflavine-bound complex were found to diminish in intensity as the temperature was increased. This observation indicates that these imino protons are exchange broadened and suggests that this region of the RNA becomes more conformationally dynamic as the temperature is increased above 283 K. The proton and nitrogen chemical shift assignments for imino resonances of RRE-IIB in the proflavine·RRE-IIB complex are given in the Supporting Information.

In contrast to the case with proflavine, the insolubility of acridine orange in aqueous buffers at NMR concentrations made formation of a stable complex between this molecule and RRE-IIB significantly more challenging. Since initial NMR results indicated that proflavine bound in a specific and unique mode and acridine orange proved not to be amenable to NMR analysis, we directed our focus on a more detailed NMR and fluorescence analysis of the interaction of proflavine with RRE-IIB.

NMR Evidence that Proflavine Binds Cooperatively to RRE-IIB as a Dimer. The nonexchangeable ^{1}H chemical shift positions from the two proflavine molecules (Figure 5A shows proflavine with ring positions labeled) in the proflavine·RRE-IIB complex were assigned using 2D TOCSY and NOESY experiments performed at 283 K on a 2:1 proflavine·RRE-IIB complex (Figure 5B−D). From a series of 2D TOCSY experiments carried out at different temperatures, it was found that proflavine in the proflavine·RRE-IIB complex showed the sharpest, most well-resolved cross-peaks at 283 K. As the temperature was increased above 283 K, the H1−H2 and H7−H8 cross-peaks broadened significantly (data not shown).

In the TOCSY spectrum (Figure 5B) of the proflavine·RRE-IIB complex at 283 K, the ^{1}H chemical shift degeneracy between protons H1 and H8 and protons H2 and H7, which is a result of the 2-fold symmetry of the free molecule, is broken for each of the bound proflavines in the proflavine·RRE-IIB complex. For convenience, the bound proflavine molecules and the corresponding resonance assignments are distinguished arbitrarily with the labels proflavine-a and proflavine-b. The TOCSY spectra provided correlations that allowed unambiguous assignment of the intramolecular H1a−H2a, H1b−H2b, H7a−H8a, and H7b−H8b positions of the bound proflavines. In addition, NOEs observed in the NOESY spectra permitted the identification of H9a and H9b as well as their assignment (Figure 5C,D). The proton chemical shift assignments for the two bound proflavines, as well as for free proflavine, are given in the Supporting Information, along with the observed chemical shift differences between the bound and free states.

The observation of two unique sets of H1−H2 and H7−H8 correlated cross-peaks in the TOCSY spectra provides strong evidence that two proflavine molecules are uniquely bound to RRE-IIB. In the bound state, the loss of chemical shift degeneracy of the proton resonances for the two proflavines would be expected on the basis of the likely asymmetry of the chemical environment provided by the RNA binding pocket. The line widths and intensities of the RNA-bound proflavine cross-peaks at 283 K were also equivalent to the widths and intensities observed for cross-peaks belonging to RRE-IIB. These equivalencies along with the breaking of degeneracy among proflavine ^{1}H chemical shifts are consistent with the specific and tight binding of two proflavine molecules in the proflavine·RRE-IIB complex. In addition, intermolecular NOEs between the two individual proflavine molecules were observed in the 2D NOESY experiments (Figure 5C,D). These NOEs unambiguously place the two uniquely bound proflavines close to each other (d_{HH} < 5 Å) and strongly suggest that the two molecules stack one above the other in the proflavine·RRE-

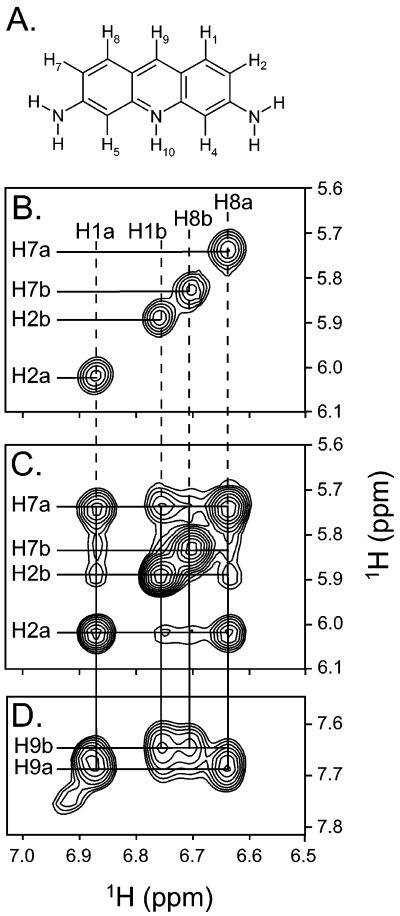

FIGURE 5: Two proflavine molecules bind to RRE-IIB and are close to each other in the bound complex. Proflavine proton chemical shifts were assigned to either of the two proflavine molecules (designated a and b) using 2D homonuclear TOCSY and NOESY spectra. (A) Proflavine structure with the ring protons numbered. (B) Expanded plot of the TOCSY experiment at 283 K showing correlations between protons H1 and H2 and protons H7 and H8 in the two proflavines, which was used to unambiguously assign the four intramolecular H1a−H2a, H1b−H2b, H7a−H8a, and H7b−H8b correlations. The four cross-peaks, two arising from each of the two proflavines bound to RRE-IIB, are labeled by the H1 and H8 proton assignments. (C) Expanded plot of the same H1−H8 to H2−H7 correlation region of a NOESY spectrum at 283 K with cross-peaks labeled according to the H2 and H7 assignments. A number of intermolecular NOEs between the two unique proflavine molecules are clearly observed in this portion of the NOESY spectrum. The observed NOE cross-peaks between proflavine-a and proflavine-b indicate that these two molecules are close to each other (d_{HH} < 5 Å) and likely stack one on top of the other in a single orientation in the bound complex. (D) Expansion of the H1/H8−H9 correlation region of the NOESY spectrum showing the unique assignment for the H9 protons from each of the bound proflavine molecules.

IIB complex. To exclude the possibility that these cross-peaks arise from a single proflavine that is in slow exchange between two bound conformational states, a 2D ROESY spectrum (data not shown) of the proflavine·RRE complex was acquired at 283 K. In the ROESY experiment, the relative sign of the cross-peaks with respect to the diagonal was used to unambiguously assign the observed cross-peaks to cross relaxation (NOE) between two proflavine molecules and not to exchange of one proflavine molecule between two bound states.

Inhibition of Formation of the Rev Peptide·RRE-IIB Complex by Proflavine. Following the observation from the

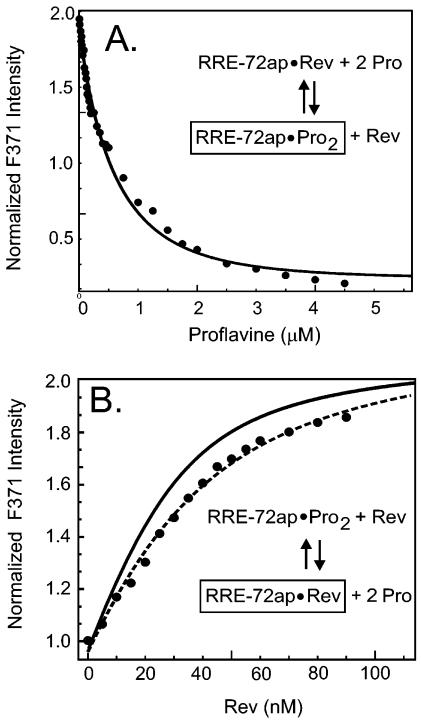

FIGURE 6: Competitive binding between proflavine and the Rev peptide for RRE-72ap. (A) Titration of a complex between RRE-72ap ($[RRE]_{tot}$ = 30 nM) and the Rev peptide ($[Rev]_{tot}$ = 60 nM) with proflavine in buffer A at 10 °C. The fit for the curve was simulated using a model in which proflavine binds competitively with the Rev peptide to a high-affinity site (K_D = 0.11 μM) and then noncompetitively with the Rev peptide for a second lower-affinity site(s) (K_D = 1.1 μM). (B) Titration of a complex between RRE-72ap ($[RRE]_{tot}$ = 30 nM) and proflavine ($[proflavine]_{tot}$ = 240 nM) with the Rev peptide (circular data points) in buffer A at 10 °C. The solid curve is a best fit to eq 1 for a titration of RRE-72ap ($[RRE]_{tot}$ = 30 nM) with the Rev peptide (data not shown), which yields a K_D of 7 ± 3 nM for Rev peptide binding under these conditions, and the dashed curve is the calculated binding isotherm if Rev peptide binding is competitive with occupation of the tight proflavine binding site (K_D = 0.104 μM). The similarity of the Rev peptide titration points (circular data points) in the presence of proflavine and the long dashed curve indicates that proflavine binding to its tight site directly competes with Rev binding to its site.

NMR experiments that proflavine binds as a dimer to a single specific site on RRE-IIB, two different competitive binding experiments were performed to determine if the interaction of proflavine with RRE was also inhibitory with respect to Rev peptide binding (Figure 6). In the first experiment, a competitive binding assay was performed in which a Rev peptide·RRE-72ap complex was titrated with increasing concentrations of proflavine (Figure 6A) under low-salt conditions (buffer A). In this experiment, the total fluorescence amplitude change is close to that expected if the fluorescence decrease due to the displacement of the Rev peptide from its site and the decrease due to proflavine binding to its intermediate binding site are additive. That is, an ~2-fold fluorescence decrease from that of the initial Rev peptide·RRE-72ap complex is expected if proflavine binding results in displacement of the Rev peptide and is silent to direct fluorescence detection with RRE-72ap, while an additional 80% decrease in fluorescence, as observed when free RRE-72ap is titrated with proflavine (Figure 3A), is expected as the proflavine saturates its intermediate binding site. From the data in Figure 6A, a K_D of 0.11 ± 0.05 μM

for proflavine binding to the competitive site was calculated by employing the simplest model in which proflavine competes with Rev peptide for binding to its tight site and then a second class of proflavines bind noncompetitively with the Rev peptide for a second weaker site(s). The two proflavine molecules, which bind with high affinity and competitively with Rev, are not resolvable in these experiments and are treated as equivalent molecules in the fitting procedure. In addition, the K_D values for the Rev peptide and the noncompetitive proflavine binding sites were held fixed at the average values of 7 nM and 1.1 μM, respectively, independently determined from fitting the direct fluorescence assays, while the K_D values for a competitive proflavine binding site and the fluorescence amplitudes were allowed to vary.

In a second set of competitive binding experiments (Figure 6B), preformed proflavine·RRE-72ap complexes were titrated with increasing concentrations of the Rev peptide. For one series of experiments carried out again in low-salt buffer conditions (buffer A), the proflavine concentration was fixed at different concentrations (60, 240, and 1000 nM) while the RRE-IIB concentration was fixed at 30 nM in all cases. In these experiments, if binding of proflavine competed with Rev peptide binding, higher apparent K_D values for Rev peptide binding should be measured as the concentration of proflavine is increased. Figure 6B shows an example of a titration of the Rev peptide with the proflavine·RRE-72ap complex, at 30 nM RRE-IIB and 240 nM proflavine. In this example, the binding curve deviates considerably from the fitted curve for Rev peptide binding to RRE-IIB in the absence of proflavine (see the solid fitted curve for a measured titration of Rev with RRE-IIB at a fixed concentration of 30 nM in Figure 6B). The Rev peptide binding curve in the presence of proflavine was fit using a displacement model in which Rev peptide and proflavine were assumed to compete directly for binding to RRE-IIB. In the fitting procedure, the K_D value of the Rev peptide was again held fixed at 7 nM, while the K_D for a competitive proflavine site and the fluorescence amplitudes were allowed to vary. The K_D determined for the competitive binding of proflavine to RRE-IIB from these fits was on average 0.11 $\pm$ 0.05 μM, and the resulting fitted curve for the 240 nM proflavine example is shown as a dashed line (Figure 6B). The titrations at other fixed concentrations of RRE-72ap and proflavine also showed apparent depressions in the Rev peptide binding affinity for RRE-IIB and could be fit using a simple displacement model. In all cases, a nanomolar competitive proflavine interaction of $\sim$100 nM affinity was calculated.

To assess the effect of more saline buffer conditions (buffer B) on the affinity observed for the competitive proflavine binding mode, the competitive binding experiment was repeated with proflavine and RRE-IIB concentrations fixed at 400 and 200 nM, respectively. In this titration experiment, the Rev peptide binding curve again deviates from the curve observed for Rev peptide binding to RRE-IIB in the absence of proflavine (data not shown). The Rev peptide binding curve in the presence of proflavine could be fit as described for the experiments carried out under lower-salt conditions using a displacement model in which the Rev peptide and proflavine were assumed to compete directly for binding to RRE-IIB. The K_D calculated for the competitive binding of proflavine to RRE-IIB from this fit was 0.15 $\pm$ 0.03 μM. Thus, although the increased salinity of the buffer mildly diminishes the affinity of proflavine for its competitive site on RRE-IIB, as would be expected on the basis of the potential electrostatic contribution to the interaction, nanomolar competitive binding is still clearly observed. Surprisingly, these results suggest there are at least two classes of proflavine binding interactions with RRE-IIB: a competitive high-affinity binding mode, which was silent in the direct binding assays, and an approximately 10-fold weaker binding mode that is suggestive of an intercalative interaction which may or may not be inhibitory with respect to Rev peptide binding. Since the Rev peptide is efficiently competed off as a result of proflavine binding at its high-affinity site, the effect on Rev binding that results from occupancy of the lower-affinity proflavine binding site(s) could not be determined.

To test whether the direct interaction of proflavine with the Rev peptide contributes in some way to the observed inhibition of Rev·RRE-IIB, the intrinsic fluorescence of proflavine was used to assay for binding to the Rev peptide. The titration of proflavine with the Rev peptide showed no detectable change in the proflavine fluorescence (data not shown), strongly suggesting that proflavine does not directly bind the Rev peptide.

Stabilization of the Purine-Rich Bulge Structure of RRE-IIB in the Proflavine·RRE-IIB Complex. To identify changes in the RRE-IIB secondary structure induced by proflavine binding, several homonuclear and ^{15}N-edited 2D NMR experiments were performed using either unlabeled or ^{15}N-labeled RRE-IIB in a 1:2 complex with proflavine. Using $^{2h}J_{NN}$ COSY and 2D ^{1}H NOESY experiments, the exchangeable imino proton resonances were assigned and the canonical base pairing schemes were established for the proflavine·RRE-IIB complex (Figure 7). The U43·G77 wobble pair provided a convenient starting point in the NOESY spectrum for establishing the "NOE walk" between imino protons observed for stacked base pairs in the lower stem of the RRE-IIB sequence. Likewise, the imino proton of U66 was used as a starting point for the sequential NOE walk through the stacked base pairs of the upper stem region which established the unambiguous assignment of the imino proton correlations up to and including G50 and G70 of the bulge region. A contiguous NOE walk throughout all of the proflavine-bound RRE-IIB was broken only at residues G47, G48, and G71, the guanine residues that can potentially form noncanonical purine·purine base pairs as previously observed in the Rev peptide·RRE-IIB complex (*27*, *29*). While three distinct imino proton resonances have been identified as belonging to G47, G48, and G71 from the NMR spectra, these resonances could not be unambiguously assigned due to the lack of observable NOEs to the neighboring bases. The $^{2h}J_{NN}$ COSY experiment confirms that two A·U and eight G·C canonical base pairs are present in the proflavine-bound form of RRE-IIB. In contrast, only two A·U and six G·C pairs, associated with the upper and lower stem of RRE-IIB, are observed in free RRE-IIB (refs *27* and *29* and data not shown). The two additional G·C base pair correlations found in the proflavine·RRE-IIB complex correlate to the G50·C69 and C49·G70 base pairs, respectively, in the bulge region of RRE-IIB. Unfortunately, no cross-peaks were identified in the $^{2h}J_{NN}$ COSY experiment which could assign

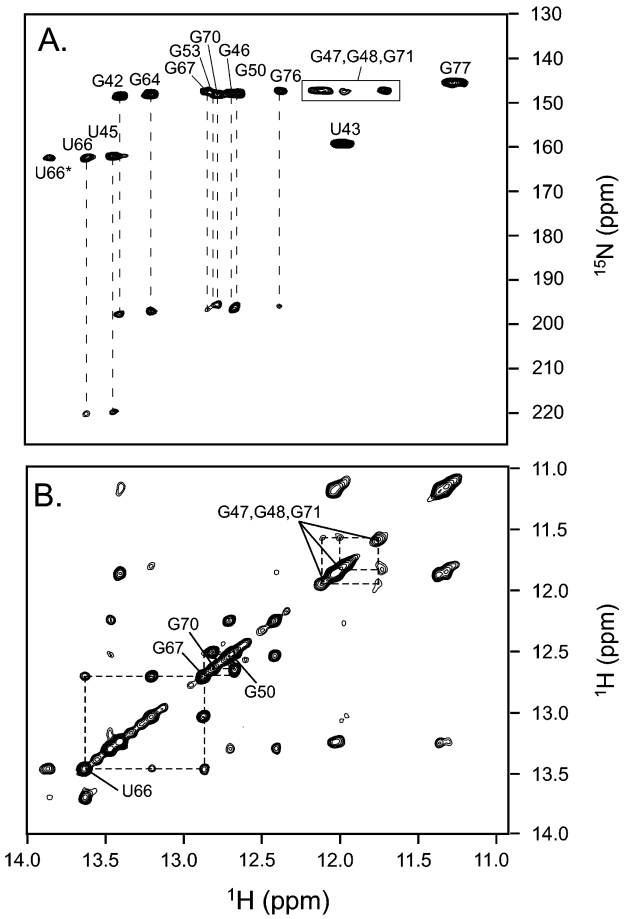

FIGURE 7: NMR spectra of the proflavine·RRE-IIB complex demonstrate that the purine-rich bulge region within RRE-IIB is stabilized by the binding of proflavine. $^{2h}J_{NN}$ COSY (*48*) and ^{1}H NOESY experiments were collected on RRE-IIB samples at 283 K. (A) Expanded plot of the $^{2h}J_{NN}$ COSY experiment with dashed lines connecting imino proton H3/N3 and H1/N1 auto peaks with the observed trans-hydrogen bond correlated cross-peaks between H3(uridine) → N1(adenine) and H1(guanosine) → N3(cytidine). Auto peaks are labeled with imino resonance assignments, and resonances belonging to residues G71, G47, and G48 which could not be unambiguously assigned are boxed. The $^{3h}J_{NN}$ trans-hydrogen bond correlations observed in the $^{2h}J_{NN}$ COSY experiment demonstrate the formation of two A·U and eight G·C base pairs in the proflavine·RRE-IIB complex, which includes the G50·C69 and C49·G70 base pairs within the bulge region of RRE-IIB. Note that the imino resonance of U66 is in slow exchange with a minor alternate conformation, designated U66*, that has been observed at lower temperatures. (B) Expansion of the region of the 2D NOESY spectrum showing imino to imino correlations, which allow sequential assignment of base pairs within stacked regions of the RNA structure. Two portions of the imino proton NOE walk through the bulge region of RRE-IIB are indicated by dashed lines and are labeled accordingly. The first trace shows NOEs among G47, G48, and G71, and the second trace shows the NOE connectivity from residue U66 in the upper stem through G50 in the bulge region of RRE-IIB.

the G47 imino resonance and confirm the presence of a purine·purine base pair involving A73.

DISCUSSION

Targeting Retroviral RNA. RNA and RNA−protein (RNP) complexes represent attractive targets for the regulation of gene expression and the treatment of retroviral and bacterial infection (*50*−*53*). For instance, modulation of RNA−protein interactions involved in transcription, messenger RNA (mRNA) processing, protein translation, or retroviral gene expression could provide novel ways of treating cancer, combating viral infection, or enhancing the effectiveness of existing chemotherapeutic and antiviral agents. In the retrovirus HIV-1, the interaction between RRE and the HIV-1 protein Rev is essential to HIV-1 replication and represents an as yet unexploited target for antiviral compound development. In this study, fluorescence and NMR binding assays have been used to select for high-affinity and specific inhibitors of the HIV-1 retroviral regulatory RNA, RRE, from a small pool of compounds that were selected by rationally directed searches of chemical compound libraries. This study demonstrates the power of a combined fluorescence screening and NMR structure-based approach to rapidly identify lead compounds that target RNA for therapeutic development. Compounds which exhibit a high-affinity association with an RNA target could be rapidly identified using the 2-AP fluorescence screen. Competitive fluorescence binding assays using the same 2-AP-labeled RRE stem−loop sequences could then be employed to determine whether a compound that is found to bind (i.e., impart a fluorescence response in the direct binding assay) might also be inhibitory with respect to Rev peptide binding. In some cases, as for proflavine, multiple binding interactions can be detected using the two fluorescence approaches. Using complementary NMR methods, compounds of interest can be further assayed for structurally interesting and/or specific binding modes. In both methodologies, we rely heavily upon modulation of RNA conformation, which is commonly observed in ligand−RNA interactions, in the design of the detection schemes for the binding event(s).

Characterization of the High-Affinity Binding Interaction of Proflavine with RRE-IIB. The NMR analysis of the proflavine·RRE-IIB complex indicates that the specific interaction of proflavine with RRE-IIB involves the binding of two proflavine molecules close to each other and in a single conformation. Since the NMR experiments were carried out under stoichiometric binding conditions and an intermediate state representing a single bound proflavine was not detected, the dimeric interaction appears to be highly cooperative and to involve two proflavine molecules with similar affinities. If the dimeric interaction were a result of occupancy first of the high-affinity binding site followed by binding to the lower-affinity site, an intermediate state of a single proflavine bound to RRE-IIB would have been expected as a result of the approximate 10-fold difference in affinity between these two binding classes. Thus, the two bound proflavines observed in the NMR experiments appear to both belong to the high-affinity binding class and bind through a highly cooperative dimeric mode.

Several 2D NOESY spectra have provided the intermolecular NOE cross-peaks that define the proximity and relative orientation of the two proflavine molecules in the bound complex. Since NOEs are observed between the two bound proflavines, it is highly unlikely that the dimeric binding mode is the result of intercalative insertion between stacked bases within RRE-IIB. Because of steric considerations, such an intercalative binding mode could involve the insertion of only one proflavine molecule between two RNA bases and would not result in the observation of direct NOEs between the two molecules. Rather, an intercalative binding mode would have likely yielded strong NOEs between

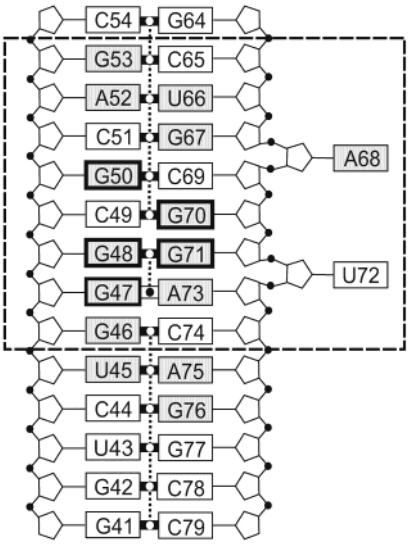

FIGURE 8: Schematic diagram of the NMR data for the proflavine•RRE-IIB complex. Bold outlines indicate bases for which imino proton resonances are observed only in the proflavine•RRE-IIB complex. Shaded boxes indicate bases for which imino proton, as well as other base proton, resonances are found to shift in the proflavine•RRE-IIB complex. Solid thick lines between boxes indicate observed imino protons in base pairs. Thin dashed lines between the circles between the bases indicate imino → imino stacking NOEs. Residues involved in high-affinity Rev peptide binding are located with the dashed line box.

proflavine and the RNA aromatic base protons. Such NOEs are not observed, although this may be due to a weakening of these NOEs by conformational dynamics at the proflavine−RRE-IIB binding interface. Instead, the observed NOEs are consistent with a structural model in which the two bound proflavine molecules are stacked one on top of each other and presumably interacting with a helical groove on the RNA. The observation of such a nonintercalative binding mode for binding of proflavine to RRE-IIB has precedent from a previous study in which multiple nonintercalative binding modes for binding of proflavine to DNA were found (*54*). In addition, a crystallographic structure of ApA with proflavine (*59*) shows that two proflavine molecules can stack upon each other and with an adenosine base.

One possible site for such a stacked dimeric interaction is the widened major groove formed upon base pairing of the purine-rich internal bulge of RRE-IIB. Such a high-affinity binding interaction of an intercalating agent with a nonduplex bulge and loop region of a nucleic acid has previously been observed in studies of both RNA (*55*−*57*) and DNA (*58*). Specific and localized binding of proflavine at the internal bulge is supported by spectral overlays of the free and proflavine-bound forms of RRE-IIB which show that the majority of the RRE-IIB imino proton chemical shifts for the helical regions outside the internal bulge do not change, while new imino proton NMR signals and changes in chemical shifts are observed for those bases associated with the internal purine-rich bulge (Figure 8). Binding at the bulge site might also be energetically favored by additional stacking of the proflavines with base A68 or U72, which can adopt extrahelical positions in the complex. However, occupancy of the high-affinity, competitive proflavine binding site is not detected in the direct titration experiments with either RRE-72ap or RRE-68ap. This indicates the conformations of the two bulge bases are not significantly different between the free and proflavine-bound RRE-IIB and are predominantly unstacked and extrahelical in both states. It also does not support a configuration in which these bases efficiently stack together with the two proflavine molecules. It should be noted that a similar lack of detectable fluorescence signal change was observed previously in titrations of the Rev peptide with RRE-68ap (*31*), where the 2-AP probe at this position of the bulge was found to be predominantly unstacked and extrahelical in both the free and Rev peptide-bound states of RRE-IIB.

In contrast to the observed competitive high-affinity interaction of proflavine with RRE-IIB, the lower-affinity interaction was found to significantly quench the fluorescence of both RRE-72ap and RRE-68ap. In this binding interaction-(s), proflavine might distort or relax the RRE-IIB bulge structure through an intercalative binding mode that results in the stacking of A68 and U72 between flanking RNA bases. The observed broadening of the NMR spectra at proflavine to RRE-IIB stoichiometric ratios of greater than 2:1 further suggests that this intermediate binding interaction is nonspecific. Nonetheless, the interaction of RRE-IIB with this secondary binding class of proflavine appears to create a unique conformation of the bulge with respect to free RRE-IIB, high-affinity proflavine-bound RRE-IIB, and Rev peptide-bound RRE-IIB structures in which these bases are on average extrahelical. An alternative explanation is that quenching of both RRE-72ap and RRE-68ap is due to a direct interaction of proflavine with these bases.

RRE-IIB Conformation in the Proflavine-Bound State. In the NMR spectra of the Rev peptide•RRE-IIB complex, the observation of correlations from additional imino proton resonances provides direct evidence that the purine-rich bulge region of RRE-IIB adopts a single conformation that is stabilized through tertiary contacts with the α-helical Rev peptide (*27*, *29*). Specifically, two Watson−Crick G•C pairs and two purine•purine base pairs in the bulge region (Figure 1) are stabilized upon binding of the Rev peptide which are not observed in the free RNA. Strikingly, the occupancy of proflavine in its high-affinity RRE-IIB site induces a similar stabilization of the bulge region and is also easily followed by monitoring changes in the imino proton resonances. In particular, two additional G•C base pairs, corresponding to the G50•C69 and C49•G70 pairs within the RRE-IIB bulge, are observed in the proflavine•RRE-IIB complex, which correspond to the same two additional G•C pairs observed in the Rev peptide•RRE-IIB complex. In addition, three additional guanosine imino correlations assigned ambiguously to G47, G48, and G71 were identified and provide indirect evidence of stabilization of noncanonical base pairs within the RRE-IIB bulge of the proflavine•RRE-IIB complex. In NOESY spectra, these three guanosine imino protons give rise to NOE cross-peaks between each other and support a model where the purine bases are paired and stacked in a contiguous fashion. A summary of the observed chemical shift changes and NOEs that define the conformational changes observed in RRE-IIB upon proflavine binding is shown in Figure 8. Although proflavine induces a significant change in the conformation and stability of the RRE-IIB bulge, this small molecule clearly does not offer the same number or kind of potential stabilizing contacts available to the Rev peptide. The lack of such stabilizing factors could account for the spectral differences observed between the

proflavine·RRE-IIB and Rev peptide·RRE-IIB complexes; most notable are the differences in the G47, G48, and G71 imino chemical shifts and the temperature sensitivity of the observed intensities for these imino protons.

Mechanism of Proflavine Inhibition of the Rev Peptide·RRE-IIB Interaction. Results from the fluorescence competitive binding assay and NMR indicate that proflavine binds tightly ($K_D = 0.11\ \mu M$) to a single specific site on RRE-IIB with a stoichiometry of 2:1 and that occupancy of this site competitively inhibits formation of the Rev peptide·RRE-IIB complex. Although the data clearly indicate that proflavine inhibits the Rev peptide by binding in a specific and nonintercalative mode, it is not certain whether interference is achieved by a direct steric effect or through a more indirect allosteric mechanism. In addition, it is important to note that direct interference and allosteric mechanisms are not mutually exclusive and could both contribute to the observed proflavine inhibition of Rev peptide binding. In the latter mechanism, the coordination of proflavine with the RNA could induce a conformational change in the bulge region which would diminish the affinity of the Rev peptide for its native binding site. Although the lack of a high-resolution structure at present prevents a definitive localization of the proflavine binding site on RRE-IIB, the enhanced stabilization of the internal bulge of RRE-IIB upon proflavine binding is highly suggestive of a direct interaction of proflavine with the internal bulge. Such an interaction would favor a competitive inhibition model in which the bound proflavine dimer simply blocks the access of the Rev peptide to its high-affinity site through direct steric inhibition. The weaker binding mode of proflavine ($K_D \sim 1\ \mu M$), which also directly affects the bulge conformation as manifested in the quenching of both 2-AP base probes in the direct titrations, may also compete with the Rev peptide. However, this inhibition is masked by the tighter binding interaction observed in the competitive fluorescence binding assays and therefore could not be measured.

Implications of the Proflavine Binding Mode for Rational Drug Design. From the NMR structural analysis of the proflavine complex with RRE-IIB, as well as the results of the fluorescence binding assays, it appears that the high-affinity interaction of proflavine may result in part from its dimeric nature. Differences in the propensity and geometry of dimer stacking among different aromatic compounds may account for the greater affinity of proflavine and certain acridine derivatives, relative to those of other polycyclic aromatic compounds. Functional groups at position 9 of the tricyclic ring, which may influence both the dimer stacking potential of these molecules and any intercalative interactions with the RNA, also appear to correlate with a significantly diminished binding affinity for RRE-IIB. These observations suggest that the competitive, high-affinity proflavine interaction may be driven primarily by hydrophobic, van der Waals, and electrostatic interactions, rather than by specific hydrogen bonding with the RNA bases. The dimeric nature of the interaction of proflavine with RRE-IIB, with two molecules likely stacked on top of each other in a single binding site, opens the possibility for designing new ligands based on covalently linking the two acridine moieties. Such linked and derivative compounds may yield not only higher affinity but also greater specificity through discrimination against intercalative as well as other nonspecific binding modes.

CONCLUSION

In this study, proflavine has been shown to bind through a specific, high-affinity dimeric interaction with RRE-IIB and to act as a competitive inhibitor of the Rev peptide·RRE-IIB complex. Since proflavine is an acridine derivative that belongs to a class of nonspecific nucleic acid intercalators, the specific binding interaction observed in this work was surprising and represents a novel example of a nonintercalative RNA binding mode for such a compound. The fact that proflavine acts as a dimer in competitively inhibiting binding of the Rev peptide to RRE-IIB opens the possibility for rational drug design based on linking and modifying proflavine and related compounds. Therefore, proflavine and related heterocyclic cationic molecules may represent a new class of compounds that could provide leads for the development of novel RNA-targeted antiviral drugs.

ACKNOWLEDGMENT

We thank Dr. F. Song for synthesis of DNA templates, Dr. T. E. Shrader (Albert Einstein College of Medicine, Bronx, NY) for generously providing plasmid (pT7-911Q) for T7 polymerase expression, and Dr. D. Brabazon (Loyola College in Maryland, Baltimore, MD) for careful reading of the manuscript.

SUPPORTING INFORMATION AVAILABLE

Proton and nitrogen chemical shifts of the imino resonances of RRE-IIB in complex with the two high-affinity proflavine molecules (Table S-I) and proton chemical shifts for free proflavine and the two uniquely bound proflavine molecules in the RRE-IIB·proflavine complex (Table S-II). This material is available free of charge via the Internet at http://pubs.acs.org.

REFERENCES

1. Daly, T. J., Cook, K. S., Gray, G. S., Maione, T. E., and Rusche, J. R. (1989) *Nature 342*, 816−819.
2. Felber, B. K., Hadzopoulouclada ras, M., Cladaras, C., Copeland, T., and Pavlakis, G. N. (1989) *Proc. Natl. Acad. Sci. U.S.A. 86*, 1495−1499.
3. Malim, M. H., Hauber, J., Fenrick, R., and Cullen, B. R. (1988) *Nature 335*, 181−183.
4. Zapp, M. L., and Green, M. R. (1989) *Nature 342*, 714−716.
5. Cochrane, A. W., Chen, C. H., and Rosen, C. A. (1990) *Proc. Natl. Acad. Sci. U.S.A. 87*, 1198−1202.
6. Malim, M. H., Freimuth, W. W., Liu, J. S., Boyle, T. J., Lyerly, H. K., Cullen, B. R., and Nabel, G. J. (1992) *J. Exp. Med. 176*, 1197−1201.
7. Duan, L., Zhu, M., Ozaki, I., Zhang, H., Wei, D. L., and Pomerantz, R. J. (1997) *Gene Ther. 4*, 533−543.
8. Zapp, M. L., Stern, S., and Green, M. R. (1993) *Cell 74*, 969−978.
9. Hendrix, M., Priestley, E. S., Joyce, G. F., and Wong, C. H. (1997) *J. Am. Chem. Soc. 119*, 3641−3648.
10. Werstuck, G., Zapp, M. L., and Green, M. R. (1996) *Chem. Biol. 3*, 129−137.
11. Wang, Y., Hamasaki, K., and Rando, R. R. (1997) *Biochemistry 36*, 768−779.
12. Cho, J. H., and Rando, R. R. (1999) *Biochemistry 38*, 8548−8554.
13. Michael, K., Wang, H., and Tor, Y. (1999) *Bioorg. Med. Chem. 7*, 1361−1371.
14. Kirk, S. R., Luedtke, N. W., and Tor, Y. (2000) *J. Am. Chem. Soc. 122*, 980−981.
15. Sucheck, S. J., Greenberg, W. A., Tolbert, T. J., and Wong, C. H. (2000) *Angew. Chem., Int. Ed. 39*, 1080.

16. Wang, H., and Tor, Y. (1998) *Angew. Chem., Int. Ed. 37*, 109−111.
17. Xiao, G., Kumar, A., Li, K., Rigl, C. T., Bajic, M., Davis, T. M., Boykin, D. W., and Wilson, W. D. (2001) *Bioorg. Med. Chem. 9*, 1097−1113.
18. Zapp, M. L., Young, D. W., Kumar, A., Singh, R., Boykin, D. W., Wilson, W. D., and Green, M. R. (1997) *Bioorg. Med. Chem. 5*, 1149−1155.
19. Ratmeyer, L., Zapp, M. L., Green, M. R., Vinayak, R., Kumar, A., Boykin, D. W., and Wilson, W. D. (1996) *Biochemistry 35*, 13689−13696.
20. Li, K., Davis, T. M., Bailly, C., Kumar, A., Boykin, D. W., and Wilson, W. D. (2001) *Biochemistry 40*, 1150−1158.
21. Chapman, R. L., Stanley, T. B., Hazen, R., and Garvey, E. P. (2002) *Antiviral Res. 54*, 149−162.
22. Kjems, J., Frankel, A. D., and Sharp, P. A. (1991) *Cell 67*, 169−178.
23. Cook, K. S., Fisk, G. J., Hauber, J., Usman, N., Daly, T. J., and Rusche, J. R. (1991) *Nucleic Acids Res. 19*, 1577−1583.
24. Kjems, J., Calnan, B. J., Frankel, A. D., and Sharp, P. A. (1992) *EMBO J. 11*, 1119−1129.
25. Tan, R. Y., Chen, L., Buettner, J. A., Hudson, D., and Frankel, A. D. (1993) *Cell 73*, 1031−1040.
26. Tan, R. Y., and Frankel, A. D. (1994) *Biochemistry 33*, 14579−14585.
27. Battiste, J. L., Tan, R. Y., Frankel, A. D., and Williamson, J. R. (1994) *Biochemistry 33*, 2741−2747.
28. Battiste, J. L., Mao, H. Y., Rao, N. S., Tan, R. Y., Muhandiram, D. R., Kay, L. E., Frankel, A. D., and Williamson, J. R. (1996) *Science 273*, 1547−1551.
29. Peterson, R. D., Bartel, D. P., Szostak, J. W., Horvath, S. J., and Feigon, J. (1994) *Biochemistry 33*, 5357−5366.
30. Peterson, R. D., and Feigon, J. (1996) *J. Mol. Biol. 264*, 863−877.
31. Lacourciere, K. A., Stivers, J. T., and Marino, J. P. (2000) *Biochemistry 39*, 5630−5641.
32. Millar, D. P. (1996) *Curr. Opin. Struct. Biol. 6*, 322−326.
33. Rist, M. J., and Marino, J. P. (2001) *Nucleic Acids Res. 29*, 2401−2408.
34. Greenberg, W. A., Priestley, E. S., Sears, P. S., Alper, P. B., Rosenbohm, C., Hendrix, M., Hung, S. C., and Wong, C. H. (1999) *J. Am. Chem. Soc. 121*, 6527−6541.
35. Mei, H. Y., Galan, A. A., Halim, N. S., Mack, D. P., Moreland, D. W., Sanders, K. B., Truong, H. N., and Czarnik, A. W. (1995) *Bioorg. Med. Chem. Lett. 5*, 2755−2760.
36. Sannes-Lowery, K. A., Mei, H. Y., and Loo, J. A. (1999) *Int. J. Mass Spectrom. 193*, 115−122.
37. Mikkelsen, N. E., Johansson, K., Virtanen, A., and Kirsebom, L. A. (2001) *Nat. Struct. Biol. 8*, 510−514.
38. Gelus, N., Hamy, F., and Bailly, C. (1999) *Bioorg. Med. Chem. 7*, 1075−1079.
39. Cho, J., and Rando, R. R. (2000) *Nucleic Acids Res. 28*, 2158−2163.
40. Krey, A., and Hahn, F. (1975) *Naturwissenschaften 62*, 99−100.
41. Ciak, J., and Fiatin, F. (1967) *Science 156*, 655−656.
42. Milligan, J. F., and Uhlenbeck, O. C. (1989) *Methods Enzymol. 180*, 51.
43. Nikonowicz, E. P., Sirr, A., Legault, P., Jucker, F. M., Baer, L. M., and Pardi, A. (1992) *Nucleic Acids Res. 20*, 4507−4513.
44. Batey, R. T., Inada, M., Kujawinski, E., Puglisi, J. D., and Williamson, J. R. (1992) *Nucleic Acids Res. 20*, 4515−4523.
45. Kuzmic, P. (1996) *Anal. Biochem. 237*, 260−273.
46. Piotto, M., Saudek, V., and Sklenar, V. (1992) *J. Biomol. NMR 2*, 661−665.
47. Lippens, G., Dhalluin, C., and Wieruszeski, J. M. (1995) *J. Biomol. NMR 5*, 327−331.
48. Dingley, A. J., and Grzesiek, S. (1998) *J. Am. Chem. Soc. 120*, 8293−8297.
49. Delaglio, F., Grzesiek, S., Vuister, G. W., Zhu, G., Pfeifer, J., and Bax, A. (1995) *J. Biomol. NMR 6*, 277−293.
50. DeJong, E. S., Luy, B., and Marino, J. P. (2002) *Curr. Top. Med. Chem. 2*, 289−302.
51. Hermann, T. (2000) *Angew. Chem., Int. Ed. 39*, 1891−1905.
52. Hermann, T., and Westhof, E. (2000) *Comb. Chem. High Throughput Screening 3*, 219−234.
53. Xavier, K. A., Eder, P. S., and Giordano, T. (2000) *Trends Biotechnol. 18*, 349−356.
54. Schelhorn, T., Kretz, S., and Zimmermann, H. W. (1992) *Cell. Mol. Biol. 38*, 345−365.
55. Wilson, W. D., Ratmeyer, L., Cegla, M. T., Spychala, J., Boykin, D., Demeunynck, M., Lhomme, J., Krishnan, G., Kennedy, D., Vinayak, R., and Zon, G. (1994) *New J. Chem. 18*, 419−423.
56. Mei, H. Y., Cui, M., Heldsinger, A., Lemrow, S. M., Loo, J. A., Sannes-Lowery, K. A., Sharmeen, L., and Czarnik, A. W. (1998) *Biochemistry 37*, 14204−14212.
57. Gayle, A. Y., and Baranger, A. M. (2002) *Bioorg. Med. Chem. Lett. 12*, 2839−2842.
58. Woodson, S. A., and Crothers, D. M. (1988) *Biochemistry 27*, 8904−8914.
59. Neidle, S., Taylor, G., Sanderson, M., Shieh, H.-S., and Berman, H. (1978) *Nucleic Acids Res. 5*, 4417.

BI034252Z